



## The use of the optical-mathematical method to describe the structure formation during friction

T.S. Skoblo<sup>1</sup>, A.I. Sidashenko<sup>1</sup>, T.V. Maltsev<sup>2\*</sup>, V.N. Romanchenko<sup>1</sup>

<sup>1</sup>Kharkiv Petro Vasylenko National Technical University of Agriculture, Kharkiv, Ukraine,

<sup>2</sup>State Enterprise "Malyshev Plant", Kharkiv, Ukraine

\*E-mail: [taras.maltsev@gmail.com](mailto:taras.maltsev@gmail.com)

### Abstract

The paper describes the two-periodicity of the compression and tension zones of the serial piston rings surfaces and hardened with a TiN/CrN multilayer ion-plasma coating after bench tests at a sliding speed of 1.3 m/s. The assessment is made from photographs of the microstructure of the surfaces of the rings. The periods of average values of negative, zero, and positive Laplacians were estimated for the columns and rows of photographs. The periods were analyzed by the initial surface and the friction zone, as well as by the general photograph of both ring variants. The result of the evaluation of individual zones revealed a significant difference between the surfaces of the ring with a multilayer ion-plasma coating, both in columns and in rows, which is associated with the wear of the effective coating layer and is confirmed by a decrease in nanohardness. Assessment of the overall photograph revealed a 30 % difference corresponding to a hardened piston ring with nanocoating with the same nature of the compression and tension zones formation, which reflects a sufficiently high resistance to plastic deformation and wear.

**Key words:** multilayer nanocoating, piston ring, friction and wear, nanohardness, optical-mathematical analysis, structure formation, plastic deformation.

### Introduction

The results of previous studies about evaluating the degree and nature of wear of serial oil scraper piston rings of the D100 diesel generator showed their insufficient wear resistance [1]. To increase their wear resistance, the authors studied the possibility of applying a hardening multilayer ion-plasma coating of the TiN/CrN system, which ensured a multiple increase in operational properties at different sliding speeds [2 - 4].

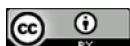
To assess the stress-strain state of various zones of serial rings during friction and hardened by an ion-plasma coating, it became necessary to use the optical-mathematical method for describing structural changes on their working surface [2, 4, 5]. This method allows to identify the relationship between the operating parameters and the formed structure in the contacting surfaces of the products, which can be estimated by approximating their digital images. Also, this method allows to assess the degree of generated stress and identify the zone of their maximum concentration [6 - 10].

After in these studies on the surfaces photographs after testing the piston rings for wear, two-periodicity of the compression and tension regions was revealed [2, 4, 5], it became necessary to describe these zones analytically.

**The aim of the study** is an analytical description of the two-periodicity of the compression and tension zones of the surfaces of serial piston rings and hardened by a TiN/CrN multilayer ion-plasma coating after bench tests at a sliding speed of 1.3 m/s from their electron-microscopic photographs of the friction surface.

### Research Methodology

To carry out the calculations, energy parameters were used and periods of average values of negative, zero, and positive Laplacians were estimated from the columns and rows of photographs of the initial surface



and the friction zone of serial (Figs. 1, 3) and hardened rings (Figs. 2, 4), respectively. Additionally, we analyzed the general images of the serial and hardened ring variants after the tests, Fig. 5, 6, respectively.

The calculation algorithm is implemented as a subroutine. The program itself sends the corresponding values to the subroutine. In each photograph (Fig. 1 - 6), the subroutine searches for the values of the each periods of its pixels in columns and rows. The cycle for trial periods was calculated in the range from 2 to 200 pixels, according to the following source data:

$s_{qj}$  – array of average values;

$s_{1j}$  – average fraction of negative Laplacians by columns or rows;

$s_{2j}$  – average fraction of zero Laplacians by columns or rows;

$s_{3j}$  – average fraction of positive Laplacians by columns or rows.

Moreover, the indices in the algorithm have the following meaning:

$q$  – the number of the sign (1 negative, 2 zero, 3 positive);

$i$  – the group number of the same trial period;

$j$  – the number inside the same group of the same trial period;

$t$  – the trial period in pixels.

The number of periods was equal to the integer part of the number of pixels divided by the period. Then, the total algebraic deviation from the average value of the fractions of negative, zero, and positive Laplacians inside the trial period was calculated using formula (1).

$$a_q = \frac{\sum_{j=1}^t s_{qj}}{t}. \quad (1)$$

The calculation of the average values of the shares of negative, zero, and positive Laplacians inside the trial period is carried out according to the formula (2).

$$b_q = \sum_{j=1}^t (s_{qj} - a_q). \quad (2)$$

After that, it was used the absolute value of the deviation from the average value according to the formula (3).

$$b_q = |b_q|. \quad (3)$$

The total value of the functional inside the trial period was found from formula (4), and from it the accumulation of functional according to formula (5).

$$c_i = b_1 + b_2 + b_3, \quad (4)$$

$$f = f + c_i. \quad (5)$$

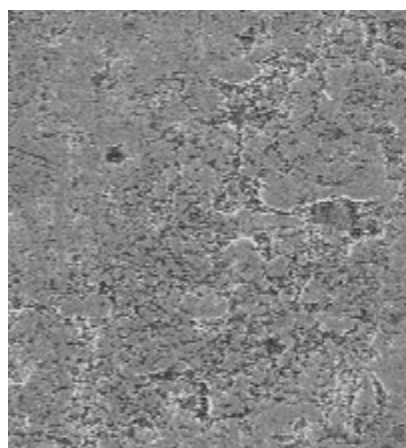


**Fig. 1. Microstructure of the initial surface of the serial ring**

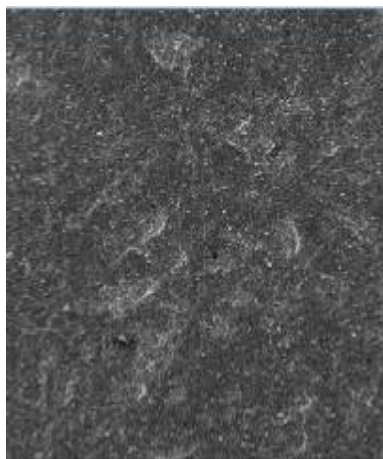


**Fig. 2. Microstructure of the initial surface of the hardened ring**

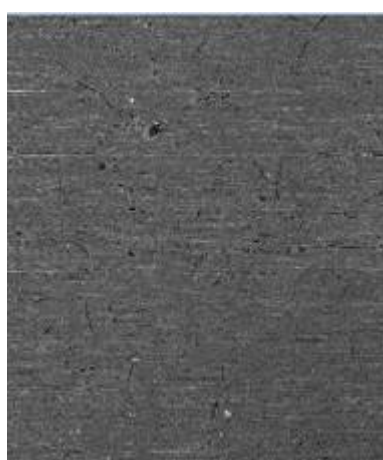


**Fig. 3. The microstructure of the friction surface of the serial ring at a sliding speed of 1.3 m/s**

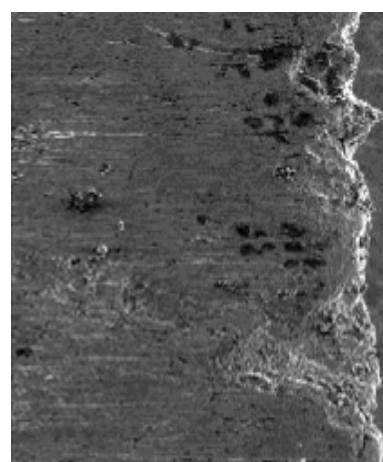


**Fig. 4. The microstructure of the friction surface of the hardened ring at a sliding speed of 1.3 m/s**

Based on the results of the cycle calculation, an array of trial periods functionals was created. The created array was sorted in descending of functionals to detect the most significant changes.

Table 1 - 4 presents the calculated periods, where the first column is the period in pixels, and the second is the corresponding functional.

As the table 1 - 4 show, the values of the functionals of both ring options differ in the results of counting in columns and in the rows of photographs of the initial and friction surfaces. However, if we compare

the functionals exclusively in rows or columns, then we can highlight a certain pattern. When counting by columns, the maximum functional of the initial surface of the serial ring is 13.7 % lower than its friction zone (see Tables 1, 3), and the hardened one is 32 % higher (see Tables 2, 4). However, a row calculation shows that the largest functional of the initial surface of a serial ring is 4 % higher than its friction zone (see Tables 1, 3), and hardened - 8.2 % lower, respectively. In both cases, both in columns and in rows, the largest difference between the surfaces is characteristic of a ring with a multilayer ion-plasma coating.

Table 1

**Values of periods and corresponding functionals  
of the initial surface photograph  
of the serial ring**

| By columns |            | By rows |            |
|------------|------------|---------|------------|
| period     | functional | period  | functional |
| 2          | 0466       | 2       | 0883       |
| 3          | 0461       | 3       | 0866       |
| 154        | 0456       | 123     | 0855       |
| 5          | 0448       | 4       | 0813       |
| 114        | 0438       | 5       | 0807       |
| 59         | 0433       | 120     | 0791       |
| 17         | 0432       | 139     | 0779       |
| 53         | 0432       | 104     | 0771       |
| 158        | 0430       | 167     | 0765       |
| 21         | 0429       | 173     | 0764       |

Table 2

**Values of periods and corresponding functionals o  
f the initial surface photograph  
of the hardened ring**

| By columns |            | By rows |            |
|------------|------------|---------|------------|
| period     | functional | period  | functional |
| 3          | 0559       | 2       | 0805       |
| 172        | 0514       | 3       | 0805       |
| 2          | 0502       | 127     | 0763       |
| 173        | 0500       | 200     | 0749       |
| 176        | 0497       | 89      | 0739       |
| 4          | 0489       | 157     | 0738       |
| 127        | 0486       | 5       | 0733       |
| 132        | 0483       | 4       | 0730       |
| 16         | 0481       | 18      | 0717       |
| 59         | 0478       | 65      | 0717       |

Table 3

**Values of periods and corresponding functionals  
of the friction surface photograph  
of the serial ring**

| By columns |            | By rows |            |
|------------|------------|---------|------------|
| period     | functional | period  | functional |
| 2          | 0540       | 3       | 0848       |
| 3          | 0526       | 2       | 0837       |
| 176        | 0508       | 4       | 0795       |
| 170        | 0499       | 152     | 0752       |
| 131        | 0491       | 93      | 0733       |
| 166        | 0474       | 5       | 0731       |
| 75         | 0471       | 95      | 0725       |
| 130        | 0468       | 136     | 0725       |
| 12         | 0467       | 164     | 0721       |
| 4          | 0465       | 33      | 0718       |

Table 4

**Values of periods and corresponding functionals  
of the friction surface photograph  
of the hardened ring**

| By columns |            | By rows |            |
|------------|------------|---------|------------|
| period     | functional | period  | functional |
| 3          | 0380       | 3       | 0877       |
| 193        | 0375       | 2       | 0831       |
| 5          | 0373       | 159     | 0767       |
| 94         | 0365       | 7       | 0764       |
| 47         | 0364       | 6       | 0760       |
| 2          | 0362       | 5       | 0742       |
| 177        | 0362       | 138     | 0740       |
| 125        | 0359       | 4       | 0728       |
| 185        | 0359       | 134     | 0722       |
| 178        | 0355       | 9       | 0718       |

This result, most likely, is associated with the wear of the effective coating layer, which is confirmed by a sharp decrease in the nanohardness of the hardened ring (initial microhardness of TiN/CrN was 53 – 59 GPa) after testing, the level of which approached the - starting material (4 - 4.7 GPa).

This is also indicated by the value of the maximum functional of the rings (calculated according to the rows of the friction zones, see Tables 2, 4).

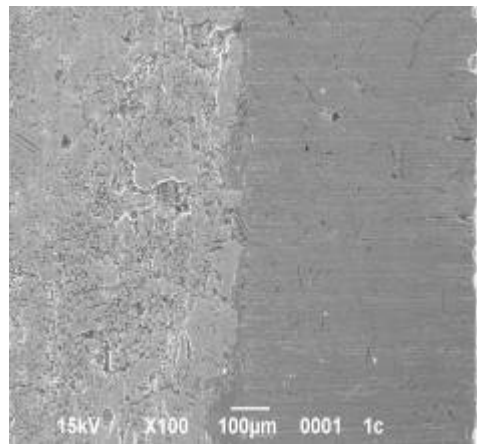


**Fig. 5. General photo of the initial (left) structure and friction surface (right) of the serial ring**

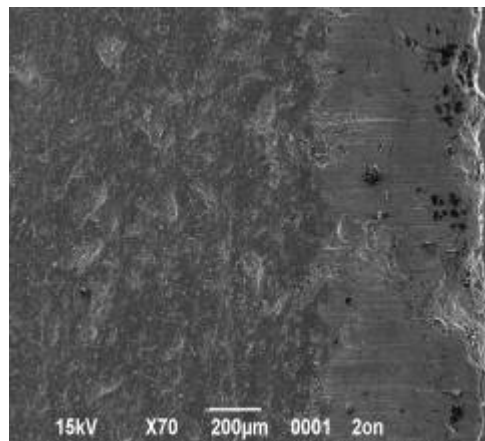


**Fig. 6. General photo of the initial (left) structure and friction surface (right) of the hardened ring**

So, on average, in columns the maximum functional of a serial ring is lower than the hardened one. The same indicator, that calculated in the rows, lower relative to the hardened ion-plasma multilayer coating of the working layer on average 30 %, which reflects its higher plastic deformation resistance in the considered directions. Moreover, the difference in columns and rows in both ring options is 26 %. This also indicates about the same distribution of compression and tension zones under identical operating conditions.

Table 5

**Values of periods and corresponding functionals  
in the general photograph  
of the serial ring after operation**

| By columns |            | By rows |            |
|------------|------------|---------|------------|
| period     | functional | period  | functional |
| 3          | 1311       | 2       | 0969       |
| 2          | 1256       | 159     | 0922       |
| 5          | 1152       | 3       | 0921       |
| 4          | 1138       | 5       | 0881       |
| 139        | 1131       | 4       | 0853       |
| 89         | 1122       | 105     | 0846       |
| 7          | 1108       | 6       | 0832       |
| 156        | 1097       | 128     | 0824       |
| 13         | 1093       | 7       | 0823       |
| 114        | 1087       | 115     | 0820       |

Table 6

**Values of periods and corresponding functionals  
in the general photograph  
of the hardened ring after operation**

| By columns |            | By rows |            |
|------------|------------|---------|------------|
| period     | functional | period  | functional |
| 3          | 1323       | 3       | 0973       |
| 2          | 1232       | 2       | 0932       |
| 4          | 1177       | 188     | 0896       |
| 5          | 1172       | 4       | 0867       |
| 175        | 1172       | 119     | 0857       |
| 182        | 1166       | 22      | 0849       |
| 103        | 1155       | 87      | 0848       |
| 7          | 1110       | 111     | 0840       |
| 116        | 1109       | 180     | 0839       |
| 114        | 1107       | 135     | 0835       |

It is possible that a high spread in the functionalities of individual ring surfaces (see Tables 1 - 4) is directly related to the separation of the general image into individual fragments. Considering that the alternation of compression and tension zones was previously recorded over the entire volume of the material of the ring working surface [5], an additional assessment was made of the functionals calculated values (Tables 5, 6) of the general photograph of both considered options (Fig. 5, 6) after testing, which show a distinctive regularity, both in rows and in columns.

### Conclusions

The studies of the nanostructured state showed the effectiveness of the proposed method for the analytical assessment of the compression and tension zones of the piston rings after friction and wear tests, namely:

- the greatest effect is achieved when calculating the functionals, the corresponding periods of the structure variability for the general picture of the working surface and the boundary in the ring;
- the revealed pattern during hardening by nanocoating reflects its rather high resistance to plastic deformation and wear;
- the difference corresponding to the variant of hardening by nanocoating of the piston ring reaches 30% with the same character of the formation process of compression and tension zones.

## References

1. Скобло Т.С. Особенности изнашивания маслосъемных поршневых колец с покрытием олова при стендовых испытаниях на трение и износ [Текст] / Т. С. Скобло, А. И. Сидашенко, Т. В. Мальцев и др. // Фізико-хімічна механіка матеріалів, м. Львів, № 4, 2017 р. – с. 71 - 77.
2. Скобло Т.С. Оптико-математический анализ моделирования структуризации упрочнённых поверхностей поршневых колец при эксплуатации [Текст] / Т.С. Скобло, А.И. Сидашенко, И.Е. Гаркуша, В.С. Таран, Р.М. Муратов, Т.В. Мальцев // Металлофизика и новейшие технологии, № 3, 2019 – с. 349 - 362.
3. Skoblo T.S. Influence of Increased Sliding Speed on the Structure and Properties of Piston Rings with Ion-Plasma Coating [Text] / T.S. Skoblo, A.I. Sidashenko, I.E. Garkusha, A.V. Taran, R.M. Muratov, T.V. Maltsev // Problems of Atomic Science and Technology, Series: Plasma Physics (118) № 6, 2018, – p. 304 - 307.
4. Скобло Т.С. Повышение стойкости поршневых колец многослойным ионно-плазменным покрытием упрочнённых поверхностей поршневых колец при эксплуатации [Текст] / Т.С. Скобло, А.И. Сидашенко, Т.В. Мальцев, В.С. Таран, Р.М. Муратов // Технология машиностроения. Специальные виды технологий, № 3, 2019 – с. 24-31.
5. Мальцев Т.В. Комплексная оценка остаточных напряжений в поршневых кольцах [Текст] / Т.В. Мальцев // «Технічний сервіс агропромислового, лісового та транспортного комплексів», м. Харків, № 10, 2017 – с. 80 - 87.
6. Скобло Т. С. Применение компьютерного анализа металлографических изображений при исследовании структуры высокохромистого чугуна [Текст] / Т. С. Скобло, О. Ю. Клочко, Е. Л. Белкин // Заводская лаборатория. Диагностика материалов, Москва, т. 78, № 6, 2012 – с. 35–42.
7. Скобло Т. С. Оценка степени неоднородности карбидов гетерогенных сплавов методом оптико-математического анализа при помощи изменчивости условных цветов [Текст] / Т. С. Скобло, О. Ю. Клочко, Е. Л. Белкин, О. И. Тришевский // Вісник ХНТУСГ ім. П. Василенка. Ресурсозберігаючі технології, матеріали та обладнання у ремонтному виробництві, Харків, Вип. 168, 2016 г. – с. 174–186.
8. Скобло Т. С. Исследование структуры высокохромистого комплекснолегированного чугуна с применением методов математического анализа [Текст] / Т. С.Скобло, О. Ю. Клочко, Е. Л. Белкин // Сталь, № 3, 2012 г. – с.46–52.
9. Тришевский О. И. Исследования микроструктур гетерогенных сплавов методом математического анализа при помощи сочетаний условных цветов и абсолютных значений лапласианов [Текст] / О. И. Тришевский, Т. С. Скобло, О. Ю. Клочко, Е. Л. Белкин // Промышленность в фокусе, Харьков, №7 (31), 2015 г. – с.52–56.
10. Скобло Т. С. Определение микротвердости структурных составляющих высокохромистых чугунов в результате математической обработки их изображений [Текст] / Т. С. Скобло, О. Ю. Клочко, Е. Л. Белкин // Вісник ХНТУСГ ім. П. Василенка. Проблеми надійності машин та засобів механізації с/г виробництва, Харків, Вип. 151, 2014 г. – с.183-189.

**Скобло Т.С., Сидашенко О.І., Мальцев Т.В.** Застосування оптико-математичного методу для опису структуроутворення при терті.

В роботі виконано опис двухперіодичності зон стиснення і розтягування поверхонь серійних поршневих кілець і, зміцнених багатошаровим іоно-плазмовим покриттям TiN/CrN після стендових випробувань при швидкості ковзання 1,3 м/с. Оцінка виконана по фотографіях мікроструктури поверхонь кілець. Були оцінені періоди середніх значень негативних, нульових і позитивних лапласіанів по стовпцях і рядках фотографій. Аналіз періодів здійснювався по вихідній поверхні і зоні тертя, а також по загальній фотографії обох варіантів кілець. Результат оцінки окремих зон виявив істотну різницю між поверхнями кільця з багатошаровим іонно-плазмовим покриттям, як за стовпцями, так і по рядках, що пов'язано зі зносом ефективного шару покриття і підтверджується зниженням нанотвердості. Оцінка загальної фотографії виявила різницю 30%, що відповідає зміцненому поршневому кільцю нанопокриттям при однаковому характері формування зон стиснення і розтягування, що відображає досить високий опір пластичній деформації і зношуванню.

**Ключові слова:** багатошарове нанопокриття, поршневі кільця, тертя і зношування, нанотвердість, оптико-математичний аналіз, структуроутворення, пластична деформація.